The effect of the solar wind on the ionosphere

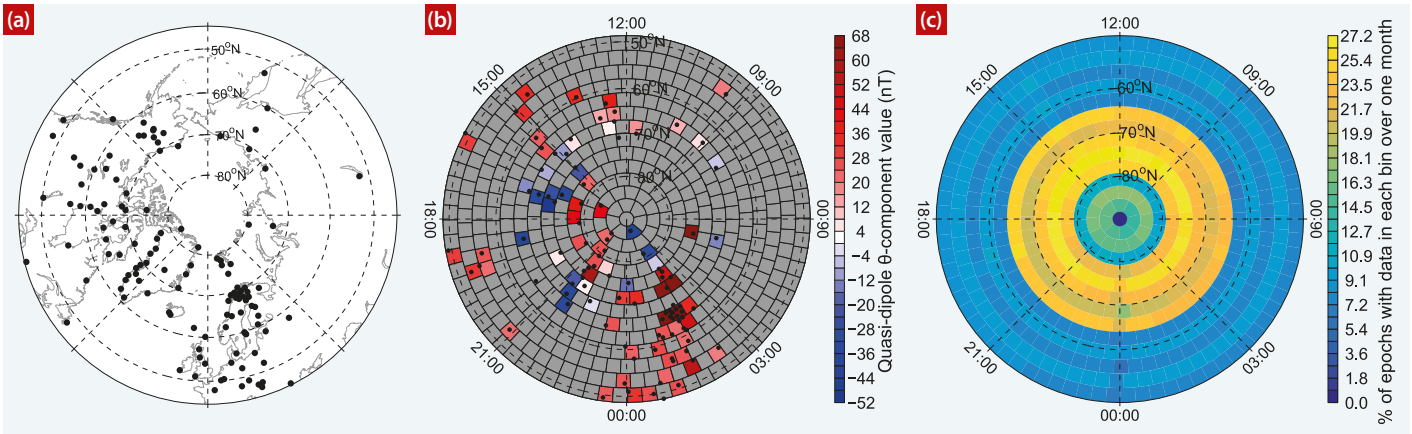

1 (a) Northern-polar geographic distribution of SuperMAG stations (black dots) which contributed measurements during February 2001. (b) The same stations at midnight on 1 February 2001, shown in quasi-dipole latitude and magnetic local time. The colours are the quasi-dipole θ component contribution on the scale shown from each station closest to the centroid of the bin it is located in, after removal of the Gjerloev (2012) long-period "year" baseline. Empty bins are grey. (c) In each locality, the percentage of 5-minute epochs to which SuperMAG contributed data over the course of the month. (Panel b from Shore *et al.* 2018)

Robert Shore describes a new, data-led technique to investigate polar geomagnetic variability, in this Rishbeth Prize-winning poster from 2018.

The outer atmosphere of the Sun envelops near-Earth space and is the ultimate control on the large-scale electrical currents that permeate our terrestrial plasma environment. These currents drive interactions both within and between the coupled ionosphere–magnetosphere system, which have wide-ranging impacts on Earth (Beggan *et al.* 2013, Knipp 2015, Pulkkinen *et al.* 2017). Studying these phenomena is of both fundamental and practical interest.

The magnetosphere covers a huge spatial scale and as a result it remains strongly undersampled. This issue of data coverage is circumvented in part by the tendency for magnetospheric dynamics to map along magnetic field lines and into the ionosphere. Thus we can think of the ionosphere acting as a projection surface for electrodynamics occurring throughout the magnetosphere (Merkin *et al.* 2016). In this way, the climatology of the large-scale electric current distribution is relatively well sampled, for instance by low Earth orbit satellites (Anderson *et al.* 2000, Friis-Christensen *et al.* 2006), and networks of ground-based magnetometers (Gjerloev 2009) and radars (Chisham *et al.* 2007).

The climatology of the ionospheric electric currents is well understood in terms of coupling to the magnetosphere, through the Dungey cycle (Dungey 1961) and the expanding/contracting polar cap paradigm (Lockwood *et. al.* 1990, Lockwood & Cowley 1991). Yet the dynamic variability of the currents has been difficult to measure and model simultaneously in all regions. This is now changing, as a result of improved access to large networks of measurement stations, combined with advances in linear and nonlinear system-scale analytic techniques. Space physics is undergoing a rapid improvement in the description of magnetosphere–ionosphere system variability. Here I report a novel combination of variance characterization techniques, with benefits for resolving the polar ionospheric magnetic fields in non-averaged terms.

Making Earth's rotation do the work

The SuperMAG archive (Gjerloev 2009, 2012) comprises decades of 1 min magnetic vector data from hundreds of contributing stations, distributed globally. The SuperMAG geographic coverage over the northern polar region is shown in figure 1a, while figure 1b shows the same distribution of stations in quasi-dipole coordinates (Richmond 1995, Emmert *et al.* 2010, Laundal & Gjerloev 2014). Here, the ionospheric magnetic fields (and their equivalent currents) are ordered in magnetic latitude and magnetic local time. In this Sun-synchronous frame, the regions of unsampled ionospheric variations are clear from the many grey patches. Yet over the course of a month, the rotation of the Earth will precess the network of stations underneath the ionosphere, leading to an overall good coverage, shown in figure 1c. Estimating the Sun-synchronous magnetic field climatology from these data is trivial: we simply compute their mean. I describe below how the method of empirical orthogonal functions (EOF) can meet the greater challenge of estimating the dynamic variability of the ionosphere in every epoch, while retaining complete spatial coverage.

EOF is a general technique; its application to geophysical fields is described mathematically in Preisendorfer and Mobley (1988), Bjornsson and Venegas (1997), Jolliffe (2002) and Storch and Zwiers (2002). The application of EOFs to SuperMAG data is described in detail by Shore *et al.* (2017, 2018). EOF uses spatial and temporal correlations within a dataset to define uncorrelated spatial and temporal "basis-vector" patterns. Each independent pattern defines the spatial regions – and their associated temporal amplitudes – which contribute the most to the total SuperMAG variability. When the patterns are ranked by their contribution to the variance, this hierarchy

shows, at a glance, the regions that are most important for describing the geomagnetic field. The sum of the EOF patterns fully describes the original data.

Each EOF basis pattern is defined across the entire spatial and temporal extent of the dataset. This means that the variations from a given pattern can be used to infer what the network would have measured in each of its data gaps, as if there had been a station there at that time. This approach is called data interpolating EOFs, and is described by Beckers and Rixen (2003) and Beckers *et al.* (2006). It is this technique that allows us to estimate the dynamic variability of the ionospheric magnetic fields without loss of spatial or temporal precision.

An interpretable parameter space

Unlike methods such as Fourier or spherical harmonic analyses, the form of the EOF patterns is unknown prior to the analysis. Indeed, discovering the morphology of these patterns is a core motivation in applying EOF to SuperMAG. Individual EOF basis patterns are defined to maximize their description of the variance of the data, so the patterns reveal directly the variance structures that make up the total dataset.

When creating a model from a given dataset, the model coefficients are typically non-unique. Because of this, we must be careful when suggesting that an inspection of the parameter space (in this case, via the EOF patterns) allows an unbiased interpretation of the underlying physical system. Campbell (2004) offers a spirited discussion of whether altering the coordinate frame of a spherical harmonic analysis, in order to better fit the underlying data, either assists or impedes physical interpretability. To be clear, the EOF patterns are orthogonal components of variability of the data; they are not necessarily individually representative of a single underlying physical phenomenon. Yet the patterns represent parts of the data that are important in terms of their contributing spatial regions and epochs. With the aforementioned shortcomings in mind, we can indeed use EOF patterns for physical interpretation.

In figure 2a, I show the EOF pattern that contributed the most to the total variance in July 2001, which resembles the two-cell ionospheric convection. The pattern is shown as a normalized map of equivalent current vectors, and its associated time series of amplitudes is shown in figure 2c. These amplitudes describe the contribution of the specific pattern shown in figure 2a to every epoch in the full dataset. In figure 2b, I show the EOF pattern that has the second highest contribution to the data variance, and its associated amplitudes in figure 2d. The patterns in figures 2a and 2b coexist in the full SuperMAG EOF decomposition.

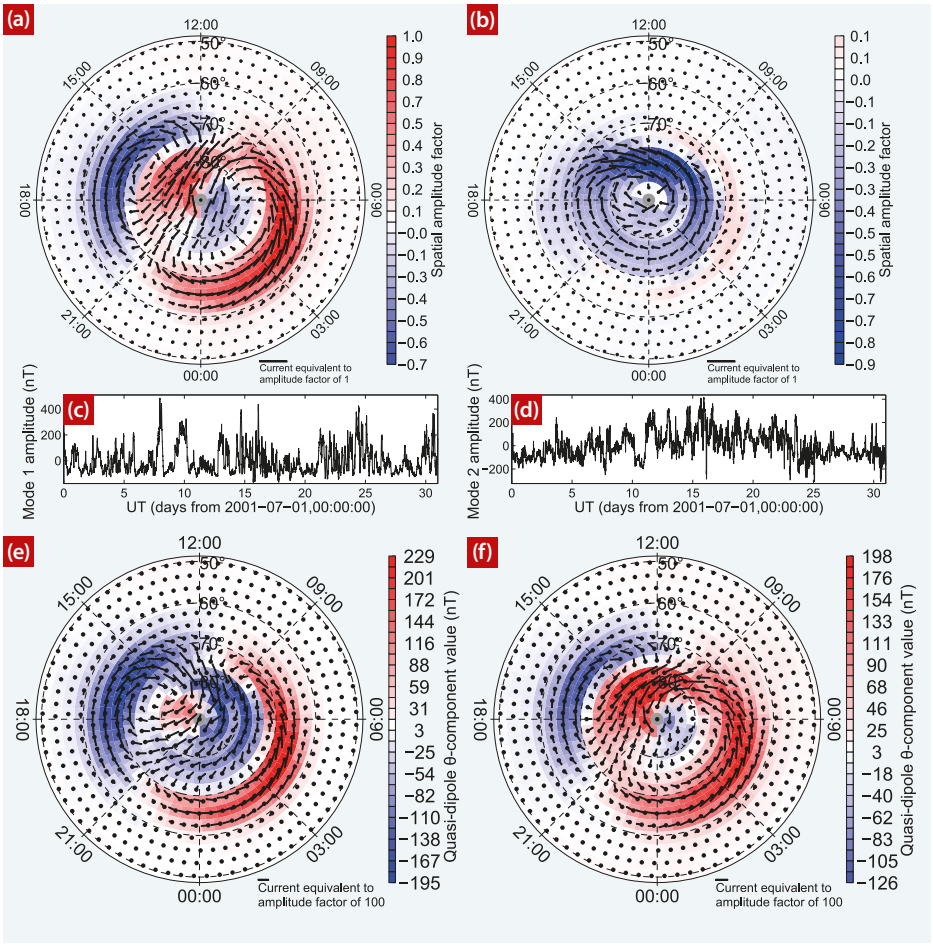

2 (a) A map of spatial amplitudes for the EOF pattern that contributed the most variance over the span of July 2001 ("mode 1" in the terminology of Shore *et al.* 2017, 2018). The vectors are the horizontal component rotated by 90° clockwise to indicate the direction and relative strength of the equivalent currents. The background colours are those of the quasi-dipole magnetic θ component. (b) The EOF pattern that contributed the second-most amount to the total July 2001 variance ("mode 2"). (c) Temporal amplitudes of the normalized pattern in (a). The mean was removed from each spatial cell prior to the EOF analysis, so the time series has zero mean. (d) Temporal amplitudes of the normalized pattern in (b). (e) Sum of (a) and (b) when they are scaled by +200 nT and –100 nT, respectively. (f) Sum of (a) and (b) when they are scaled by +200 nT and +250 nT respectively. (Using data from Shore *et al.* 2018)

There are many more EOF patterns in this month alone (not shown here).

While each individual EOF pattern is a linear representation of just one part of the geomagnetic field, their sum returns the full nonlinear behaviour of the data. So, the sum of the patterns in figures 2a and 2b, with different relative amplitudes and signs, will create a dynamic variation in the map of geomagnetic perturbations. This is demonstrated in figures 2e and 2f. Here, the pattern in figure 2a is scaled with a fixed amplitude of +200 nT, to which is added the pattern in figure 2b after scaling either with an amplitude of –100 nT (to produce figure 2e) or +250 nT (to produce figure 2f). The result is a distortion of the two-cell convection to produce the "banana" and "orange" cell patterns associated (Tenfjord *et al.* 2015) with the east–west component ($\mathbf{B}_y$) of the interplanetary magnetic field (IMF). Indeed, the time series in figure 2d has a correlation of 0.75 with the IMF $\mathbf{B}_y$ measurements.

A practical motivation for using EOF is that it can provide a compact representation of data, requiring few basis vectors to represent the geomagnetic field dynamics. If we were to use nonlinear basis vectors, such as those employed in machine learning, then the description would be even more compact and accurate, but we would be unable to interpret the individual basis vectors physically. The focus of my recent work has been to combine the benefits of EOF with other data representation techniques, in order to give a fuller picture of the spatial and temporal scales of the geomagnetic field variability.

Characterizing variability in space and time

Grocott and Milan (2014) have shown that time series of individual spherical harmonic coefficient amplitudes can be used to infer the effect of the IMF on ionospheric convection. Shore *et al.* (2017) showed that the EOF decomposition produces patterns that represent the solar wind driving more directly than individual spherical harmonics do – as expected, because the IMF has

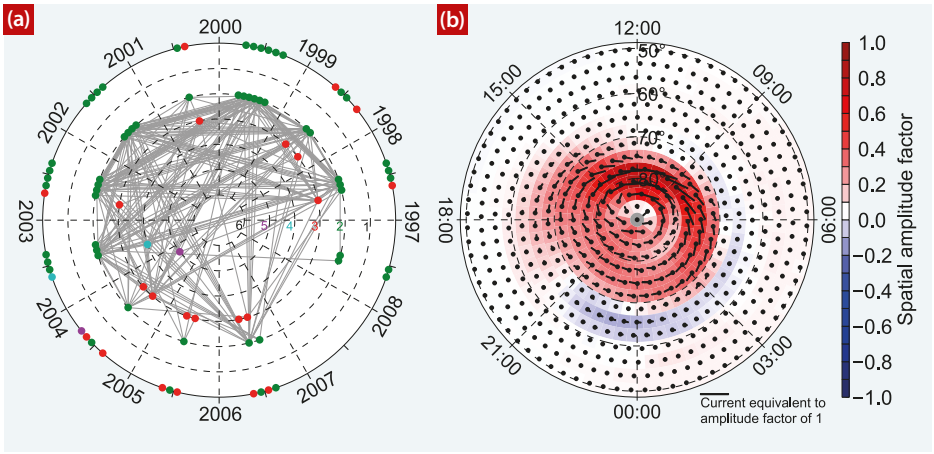

3 (a) Clustering (in time and ranked variance) of a group of EOF patterns with similar morphology, identified by Shore *et al.* (2018). The angle around the circle indicates the year and monthly analysis date. Each coloured dot indicates an EOF pattern from a given monthly analysis. The dot's placement on the dashed concentric circles indicates that pattern's contribution to the total variance (also indicated by colour) – the sixth most important pattern is innermost. The outermost (solid) circle shows all dots for the group, such that their temporal dependence is more easily visible. The grey lines indicate patterns that share a high spatial similarity (correlation coefficient ≥0.835). (b) The mean spatial pattern of all dots in (a), shown in the same format as in figure 2a and 2b. (Modified from Shore *et al.* 2018)

a strong control on ionospheric variability (figure 2). But the extent to which the EOF patterns describe the same solar wind driving varies between different monthly EOF analyses. As I show below, the information selectively represented by EOF can also offer insight into solar–terrestrial coupling. To characterize the information content – and deficit – of EOF analyses over a complete solar cycle, Shore *et al.* (2018) developed a combination of EOF with network analysis (Caldarelli 2007) and linear correlation.

"This approaches a full description of the polar geomagnetic variability"

Much in the same way that EOF analysis uses spatiotemporal covariance to resolve independent yet coexistent patterns in a dataset, network analysis identifies independent coexistent groups, based on some Euclidian distance measure of similarity within a dataset. These techniques are naturally complementary: EOF is used to identify uncorrelated patterns within a given month, then network analysis identifies correlated similarities in the EOF pattern hierarchy between independent months. Shore *et al.* (2018) performed 144 monthly EOF analyses spanning 1997.0 – 2009.0, and subsequently used network analysis to identify spatially similar clusters of EOF patterns. Here, the distance measure was spatial correlation of the EOF patterns (described in full in Shore *et al.* 2018).

In figure 3a, I show one of the coexistent groups identified by Shore *et al.* (2018). Each dot is an EOF pattern of shared spatial similarity. The mean spatial pattern from these months is shown in figure 3b, and is similar (after a sign change) to the pattern shown in figure 2b. Likewise for figure 2d, the correlation between IMF $\mathbf{B}_y$, and of each of the monthly time series indicated by the dots in figure 3a is consistently good (maximum 0.82, mean 0.63). From this result, and from established theory (Friis-Christensen & Wilhjelm 1975, Tenfjord *et al.* 2015) the group shown in figure 3a is considered to represent the IMF $\mathbf{B}_y$ input to the ionosphere. We see that the group is dominant in summer solstice and at solar maximum, and that its constituent EOF patterns tend to decrease in their relative contribution to the total variance away from summer solstice. This is indicated by the variance ranking of the group's constituent patterns slipping from second (at solstice) to third, fourth or fifth place. The IMF $\mathbf{B}_y$ driving is absent in winter.

The aim of this example is to show how the importance of this pattern (and, hence, the IMF $\mathbf{B}_y$ driving) waxes and wanes with time at a monthly granularity. On finer scales, the five-minute resolution of the EOF patterns, which make up this group, quantifies the relative importance of the IMF $\mathbf{B}_y$ driving at every epoch. In this way, the combination of EOF and network analysis, with linear correlation, allows the dynamic contribution from a specific class of solar wind driving to be quantified at a high temporal resolution, and also in terms of its spatial distribution.

In addition to the group described above, Shore *et al.* (2018) defined groups that identify the ionospheric response to positive and negative IMF $\mathbf{B}_z$, substorms, and the expansion and contraction of the polar cap. Collectively, this information approaches a full description of the polar geomagnetic variability. The quantification of the relative importance of all these aspects, both in space and time, is a step towards accurately representing the full ionospheric response to the solar wind.

Conclusion

Space physics and solar–terrestrial science is increasingly "data driven" in response to the ever-increasing quantity of easily available, high-quality network data. To make best use of these datasets, we need new techniques for the description and understanding of near-Earth electromagnetic processes. One such technique is a combination of empirical orthogonal functions, network analysis and linear regression, described above. In combination, these methods allow a meaningful interpretation of the "structures" of variability that characterize how the ionosphere and magnetosphere interact on a broad range of spatial and temporal scales. This new overview provides the information required to improve the nowcasting, forecasting and hindcasting of solar–terrestrial coupling. ●

AUTHOR

Robert Shore is a postdoctoral research associate at the British Antarctic Survey, Cambridge, UK.

RISHBETH PRIZE

This work was awarded a Rishbeth Prize for the best student poster at the Spring MIST Meeting in Southampton in 2018. The Rishbeth Prizes are awarded annually; they remember Henry Rishbeth, founder of MIST with Peter Kendall.

REFERENCES

Anderson B J *et al.* 2000 *Geophys. Res. Letts* **27**(24) 4045
Beckers J M & Rixen M 2003 *J. Atmos. Oceanic Tech.* **20**(12) 1839
Beckers J M *et al.* 2006 *Ocean Sci.* **2**(2) 183
Beggan C D *et al.* 2013 *Space Weather* **11**(7) 407
Bjornsson H & Venegas S 1997 *CCGCR Report* **97** 1
Caldarelli G 2007 *Scale-free Networks: Complex Webs in Nature and Technology* (Oxford University Press)
Campbell W H 2004 *Eos Trans. AGU* **85**(37) 350
Chisham G *et al.* 2007 *Surveys in Geophysics* **28**(1) 33
Dungey J W 1961 *Phys. Rev. Letts* **6**(2) 47
Emmert J T *et al.* 2010 *J. Geophys. Res.: Space Physics* **115**(A8) A08322
Friis-Christensen E & Wilhjelm J 1975 *J. Geophys. Res.* **80**(10) 1248
Friis-Christensen E *et al.* 2006 *Earth Planets and Space* **58**(4) 351
Gjerloev J W 2009 *Eos Trans. AGU* **90**(27) 230
Gjerloev J W 2012 *J. Geophys. Res.: Space Physics* **117** A09213
Grocott A & Milan S E 2014 *J. Geophys. Res.: Space Physics* **119**(7) 5861
Jolliffe I T 2002 *Principal Component Analysis* (Springer, New York)
Knipp D J 2015 *Space Weather* **13**(11) 742
Laundal K M & Gjerloev J W 2014 *J. Geophys. Res.: Space Physics* **119**(10) 8637
Lockwood M & Cowley S 1992 *Proceedings of the International Conference on Substorms ICS-1* (EAS)
Lockwood M *et al.* 1990 *J. Geophys. Res.: Space Physics* **95**(A6) 7961
Merkin V G *et al.* 2016 *Space Weather* **14**(2) 165
Preisendorfer R W & Mobley C D 1988 *Principal Component Analysis in Meteorology and Oceanography* (Elsevier, Amsterdam, New York)
Pulkkinen A *et al.* 2017 *Space Weather* **15**(7) 828
Richmond A D 1995 *J. Geomagnetism and Geoelectricity* **47**(2) 191
Shore R M *et al.* 2017 *J. Geophys. Res: Space Physics* **122** 2440
Shore R M *et al.* 2018 *J. Geophys. Res: Space Physics* **123** 781
Storch H v & Zwiers F W 2002 *Statistical Analysis in Climate Research* (Cambridge University Press, Cambridge)
Tenfjord P *et al.* 2015 *J. Geophys. Res.: Space Physics* **120**(11) 9368